A π/4 Compact Polarimetric Model for High-Resolution Radar in Target Recognition

Liang Zhang[*], Suixue Wang[*], Yu Wang[*], Yin Xiang[*], Junfu Wang[†], Yanhua Wang[* ‡], Yang Li[*]
[*] Beijing Key Laboratory of Embedded Real-time Information Processing Technology,
School of Information and Electronics, Beijing Institute of Technology, Beijing, China
[†] Beijing Racobit Electronic Information Technology Co. Ltd., Beijing, China
[‡] Email: wyhlucky@bit.edu.cn

Abstract: Polarimetric information can fully reflect the electromagnetic scattering characteristics of radar target. Compact polarization, which can reduce the system complexity while preserving the polarimetric information, has become an important technique of getting polarimetric information in recent years. In this paper we propose a modified implementation for π/4 compact polarimetric mode radar, where the transmitter polarization is orientated at 45°, and the receivers are at 45° and 135° polarizations. A procedure of reconstructing the full polarimetric information and extracting the features are subsequently deduced. From experimental data, we verify the scheme can distinguish different polarimetric scattering mechanisms. The method shows potential to better reconstruct fully polarimetric data and application value in target recognition.

Keywords: polarimetric radar; high-resolution radar; compact polarization; target recognition

I. Introduction

Polarization, together with the amplitude and phase, completes the electromagnetic scattering information that can be obtained on target returns. Exploiting polarimetric information can enhance the performances of detection, recognition and anti-interference. Thus, polarization acquisition and information processing have become a promising research field in radar systems [1], [2].

Polarimetric radar systems can be divided into three categories: dual-polarization, full-polarization and compact-polarization. Dual polarimetric (dual-pol) radar, which transmits a single polarization and receives two orthogonal polarizations simultaneously, obtains only one column of scattering matrix [3]. Full polarimetric (full-pol) radar allows derivation of the whole scattering matrix by transmitting two orthogonal polarizations alternately or simultaneously, but at the cost of increasing the hardware complexities [4]. Compact polarimetric (CP) radar is a modified dual polarimetric radar that has the potential to reconstruct the full scattering matrix [5]. There are currently three compact-polarization configurations. The $\pi/4$ mode transmits a 45° linear polarization and receives horizontal (H) and vertical (V) polarizations. The dual circular mode transmits a right or left circular polarization and receives both. The circular transmit/linear receive mode transmits a right or left circular polarization and receives H and V polarizations.

In this paper, we present a modified configuration for $\pi/4$ CP mode radar. It transmits a 45° linear polarization and receives 45° and 135° linear polarizations. This can be achieved by simply rotating a dual-pol radar around the line of sight. The reconstruction of the pseudo quad data is derived based on the conventional $\pi/4$ mode. We also evaluate the potentials of the proposed configuration on radar target recognition using high range resolution profiles (HRRP). The scattering entropy and scattering angle are extracted as the features. Experimental results demonstrate its capability of distinguishing different polarimetric scattering mechanisms.

This paper is structured as follows. Section 2 introduces the implementation of the proposed configuration and describes the procedure of estimating full polarimetric (FP) information from this design. In Section 3, the extraction of two polarimetric features (scattering entropy and scattering angle) is introduced. Experimental results are provided in Section 4, and the whole paper is concluded in Section 5.

II. System Model

A. System Configuration

This paper explores a modified configuration for $\pi/4$ CP mode based on dual-pol radar. Rotating the antenna around the line of sight by 45°, the transmitting polarization is changed from H polarization to 45° linear polarization, and the two receiving polarizations are changed from H and V polarizations to 45° and 135° linear polarizations. The transmitting and receiving polarizations of this mode are shown in Fig. 1. The polarimetric information is better preserved than traditional dual-pol mode without the need of an orthogonal polarimetrc transmitting path.

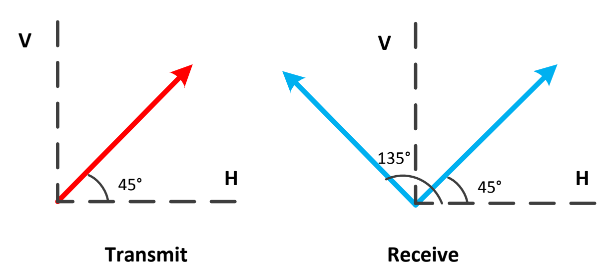

Fig. 1. Transmitting and receiving linear polarizations.

This work was supported by the Chang Jiang Scholars Programme (Grant No. 2012122) and the Hundred Leading Talent Project of Beijing Science and Technology (Grant No. Z141101001514005).

B. Signal Model

The polarization measurement vector is given by

$$\vec{k} = PS\vec{J} \tag{1}$$

where $\vec{k}$ and $\vec{J}$ are receiving and transmitting polarization vectors, respectively. P is the transformation matrix defined by different polarization bases, and S is the polarimetric scattering matrix (PSM) of the target, i.e.,

$$S = \begin{bmatrix} S_{hh} & S_{hv} \\ S_{vh} & S_{vv} \end{bmatrix}. \tag{2}$$

In the proposed configuration, the transmitting polarization vector $\vec{J}_{\pi/4}$ and the transformation matrix P from the H-V basis to the 45°-135° basis can be expressed as follows:

$$\vec{J}_{\pi/4} = \frac{1}{\sqrt{2}}\begin{bmatrix} 1 \\ 1 \end{bmatrix}, \quad P = \begin{bmatrix} 1 & 1 \\ 1 & -1 \end{bmatrix}. \tag{3}$$

Accordingly, the receiving polarization vector $\vec{k}_{\pi/4}$ is then given by

$$\vec{k}_{\pi/4} = PS\vec{J}_{\pi/4} = \frac{1}{\sqrt{2}}\begin{bmatrix} S_{hh} + S_{hv} + S_{vh} + S_{vv} \\ S_{hh} + S_{hv} - S_{vh} - S_{vv} \end{bmatrix}. \tag{4}$$

In the mono-static case, due to the reciprocity of PSM ($S_{vh} = S_{hv}$), $\vec{k}_{\pi/4}$ is simplified to

$$\vec{k}_{\pi/4} = \frac{1}{\sqrt{2}}\begin{bmatrix} S_{hh} + 2S_{hv} + S_{vv} \\ S_{hh} - S_{vv} \end{bmatrix}. \tag{5}$$

It follows that the measurement vector is a linear combination of co-polarized (co-pol) and cross-polarized (X-pol) response of the target.

C. CP Covariance Matrix

The compact polarimetric covariance matrix $C_{\pi/4}$ is defined by

$$\begin{aligned} C_{\pi/4} &= \left\langle \vec{k}_{\pi/4} \cdot \vec{k}_{\pi/4}^{H} \right\rangle \\ &= \frac{1}{2}\begin{bmatrix} H + V + 2\,\mathrm{Re}\{P\} & H - V - 2\,\mathrm{Im}\{P\} \\ H - V + 2\,\mathrm{Im}\{P\} & H + V - 2\,\mathrm{Re}\{P\} \end{bmatrix} + \frac{1}{2}\begin{bmatrix} 4X & 0 \\ 0 & 0 \end{bmatrix} \\ &+ \frac{1}{2}\begin{bmatrix} 4\,\mathrm{Re}\{\langle xh^* \rangle\} + 4\,\mathrm{Re}\{\langle xv^* \rangle\} & 2\left(\langle xh^* \rangle - \langle xv^* \rangle\right) \\ 2\left(\langle xh^* \rangle - \langle xv^* \rangle\right)^* & 0 \end{bmatrix} \end{aligned} \tag{6}$$

where symbol <·> denotes the spatial averaging operation. The notations h, x and v are substituted to S_{hh}, S_{hv} and S_{vv}, respectively, and H, V, X, P to $\langle |S_{hh}|^2 \rangle$, $\langle |S_{vv}|^2 \rangle$, $\langle |S_{hv}|^2 \rangle$ and $\langle S_{hh} \cdot S_{vv}^* \rangle$. The constant term does not influence the polarimetric information, thus it is ignored in the following deduction.

D. Reconstruction of FP Covariance Matrix

In the mono-static case, the FP measurement is characterized by the complex target vector:

$$\vec{k}_{FP} = \begin{bmatrix} S_{hh} & \sqrt{2}S_{hv} & S_{vv} \end{bmatrix}^T \tag{7}$$

and the FP covariance matrix is then given by

$$C_{FP} = \left\langle \vec{k}_{FP} \cdot \vec{k}_{FP}^{H} \right\rangle = \begin{bmatrix} H & \sqrt{2}\langle hx^* \rangle & P \\ \sqrt{2}\langle xh^* \rangle & 2X & \sqrt{2}\langle xv^* \rangle \\ P^* & \sqrt{2}\langle vx^* \rangle & V \end{bmatrix}. \tag{8}$$

In order to estimate the unknown parameters in (8) from (6), two assumptions are required.

1) Reflecting Symmetry Condition of Radar Target. The co-pol and X-pol terms are completely uncorrelated [6]:

$$\langle hx^* \rangle = \langle xv^* \rangle = 0. \tag{9}$$

2) Constraint of X-pol to co-pol Ratio and co-pol Correlation Coefficient. There is a simplified constraint of X-pol to co-pol ratio $X/(H+V)$ and co-pol correlation coefficient ρ:

$$\frac{X}{H+V} = \frac{1-|\rho|}{N} \tag{10}$$

where co-pol correlation coefficient ρ is defined by

$$\rho \equiv \frac{P}{\sqrt{HV}}. \tag{11}$$

Based on the above two assumptions, an iterative algorithm is derived to reconstruct C_{FP} from $C_{\pi/4}$.

Step1: Initialization. The initial value of ρ and X are both zeros, i.e.,

$$\begin{aligned} \rho^{(0)} &= 0 \\ X^{(0)} &= 0. \end{aligned} \tag{12}$$

Step2: ρ-step. In each iteration, ρ is updated by

$$\rho^{(k)} = \frac{C_{11} - C_{22} + C_{21} - C_{12} - 4X^{(k-1)}}{\sqrt{\left(W_1 - 4X^{(k-1)}\right)\left(W_2 - 4X^{(k-1)}\right)}} \tag{13}$$

where $W_1 = C_{11} + C_{22} + C_{21} + C_{12}$, $W_2 = C_{11} + C_{22} - C_{21} - C_{12}$.

Step3: X-step. According to (10), let the initial value of N equal 4 [5], and X is updated by

$$X^{(k)} = \frac{\left(C_{11} + C_{22}\right)\left(1 - \left|\rho^{(k-1)}\right|\right)}{2N + 4\left(1 - \left|\rho^{(k-1)}\right|\right)}. \tag{14}$$

Step4: Do the iterative process until X and ρ both converge. Then the estimation of H, P, V is given by (15), (16) and (17):

$$H = \frac{1}{4}\left(C_{11} - 4X + C_{12} + C_{21} + C_{22}\right) \tag{15}$$

$$P = \frac{1}{4}\left(C_{11} - 4X - C_{22} + C_{21} - C_{12}\right) \tag{16}$$

$$V = \frac{1}{4}\left(C_{11} - 4X + C_{22} - C_{12} - C_{21}\right) \tag{17}$$

Using these three parameters, we can estimate N again:

$$N = \frac{H + V - 2\,\mathrm{Re}(P)}{X}. \tag{18}$$

Step5: Replace the N in (14) with the new one in (18), and perform the iterative algorithm from step1 to step4 again to get the more accurate estimation of X, H, P and V.

Step6: Finally, the estimate of the FP covariance matrix under the two assumptions mentioned preciously is given by

$$\hat{C}_{FP} = \begin{bmatrix} H & 0 & P \\ 0 & 2X & 0 \\ P^* & 0 & V \end{bmatrix}. \tag{19}$$

III. Polarization Features Extraction

In 1997, Cloude *et al* proposed a classification scheme by using scattering entropy H_e and scattering angle α, which are calculated from eigenvalues and eigenvectors of the coherency matrix T_{FP} [7]. In this paper, T_{FP} can be obtained from $\hat{C}_{FP}$:

$$T_{FP} = \frac{1}{2}\begin{bmatrix} 1 & 0 & 1 \\ 1 & 0 & -1 \\ 0 & \sqrt{2} & 0 \end{bmatrix} C_{FP} \begin{bmatrix} 1 & 1 & 0 \\ 0 & 0 & \sqrt{2} \\ 1 & -1 & 0 \end{bmatrix}. \tag{20}$$

T_{FP} is a Hermitian matrix that has the following factorization:

$$T_{FP} = U \Lambda U^{-1} \tag{21}$$

where Λ is a diagonal matrix containing three real eigenvalues, and U is a unitary matrix containing three orthogonal eigenvectors. Each eigenvector has the following form:

$$\vec{e}_i = \begin{bmatrix} e_{1i} \\ e_{2i} \\ e_{3i} \end{bmatrix} = \begin{bmatrix} \cos\alpha_i e^{i\Psi_{1i}} \\ \sin\alpha_i \cos\beta_i e^{i\Psi_{2i}} \\ \sin\alpha_i \cos\beta_i e^{i\Psi_{3i}} \end{bmatrix}. \tag{22}$$

The entropy H_e is defined by

$$H_e = -\sum_{i=1}^{3} P_i \log_3(P_i) \qquad P_i = \frac{\lambda_i}{\sum_{i=1}^{3}\lambda_i}. \tag{23}$$

H_e describes the randomness of scattering and satisfies $0 \le H_e \le 1$.The scattering angle α_i is defined as:

$$\alpha_i = \arccos(|e_{1i}|). \tag{24}$$

The mean of these three angles can describe the type of scattering mechanisms:

$$\alpha = P_1\alpha_1 + P_2\alpha_2 + P_3\alpha_3, \quad 0 \le \alpha \le 90°. \tag{25}$$

We use a two-dimensional plane composed by H_e and α to classify different scattering mechanisms of radar targets. There are 9 types of scattering mechanisms in the $H-\alpha$ space as shown in Fig. 2 [7].

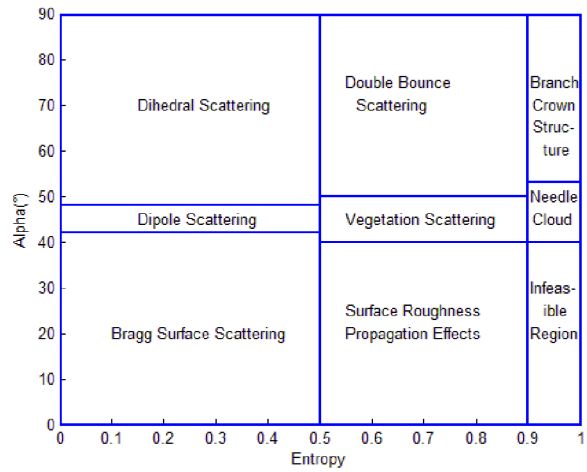

Fig. 2. Nine zones in $H-\alpha$ space.

IV. Experimental Results

A. Point Targets

We used the proposed $\pi/4$ CP mode to measure polarimetric information of a dihedral and a trihedral corner reflector. The transmitted signal was stepped-frequency linear frequency modulated (SFLFM) signal and the synthetic bandwidth was 1250MHz. The dihedral and trihedral corner reflectors represent two different typical scattering mechanisms: double-bounce scattering and odd-bounce scattering.

Fig. 3 shows the HRRPs of the two corner reflectors which are measured in the proposed $\pi/4$ CP mode and Fig. 4 shows the HRRPs of HH, VH, HV and VV polarization after reconstruction of these two corner reflectors (i.e., $|S_{hh}|$, $|S_{vh}|$, $|S_{hv}|$ and $|S_{vv}|$, which are computed from the reconstruction results H, X and V). Note that each range cell represents 0.09375 meter in figures.

Table I shows the entropy and alpha of these two corner reflectors including theoretical values and experimental results. It demonstrates a good consistency between the theoretical values and the experimental results. It can be also seen that the proposed scheme is able to effectively distinguish different scattering mechanisms of dihedral and trihedral corner reflectors from the feature α.

TABLE I. Entropy And Alpha of Corner Reflectors

	Dihedral		**Trihedral**	
	H_e	α (°)	H_e	α (°)
Experimental value	0.004	86.71	0.001	2.52
Theoretical value	0	90	0	0

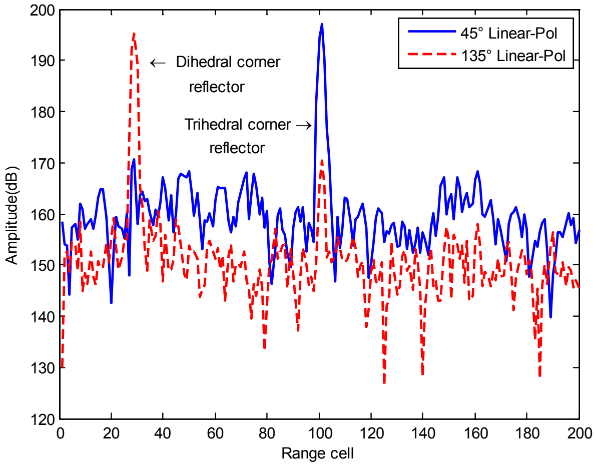

Fig. 3. Polarimetric HRRPs of corner reflectors.

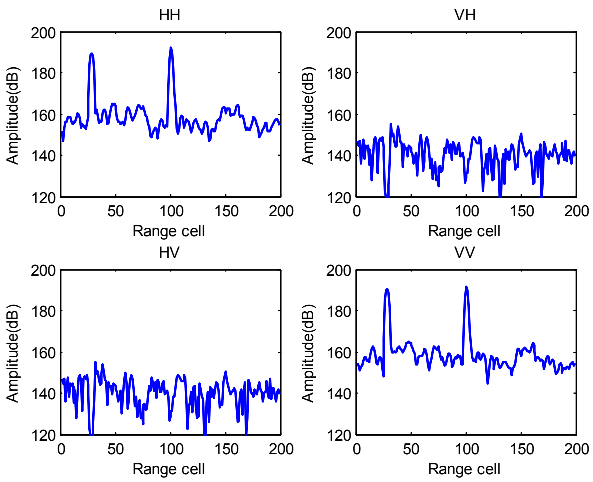

Fig. 4. Reconstruction results of corner reflectors.

B. Volume Targets

We also measured polarimetric information of two volume targets: a van and a transmission tower. Fig. 5 shows the pictures of the targets and Fig. 6 shows the HRPPs. Table II shows the statistical distribution of every range cell of nine different zones in $H-\alpha$ space. It can be seen that the scattering mechanisms of transmission tower are mainly dihedral and bragg scattering, where the highest proportion of dihedral scattering is approaching 40%. The main scattering type of van is bragg scattering whose proportion is nearly 65%, and the proportion of dihedral scattering type is only less than 5%. Therefore, this scheme is able to recognize these two volume targets effectively by contrasting the proportion of different scattering mechanisms.

V. Conclusion

In this paper we have introduced an implementation of π/4 compact polarimetric mode for high-resolution radar and shown the procedure of full polarimetric parameters estimation and features extraction. Experimental results from point and volume target validated the proposed scheme and suggests that the scheme has a good potential in target recognition.

Fig. 5. Physical pictures of van and transmission tower.

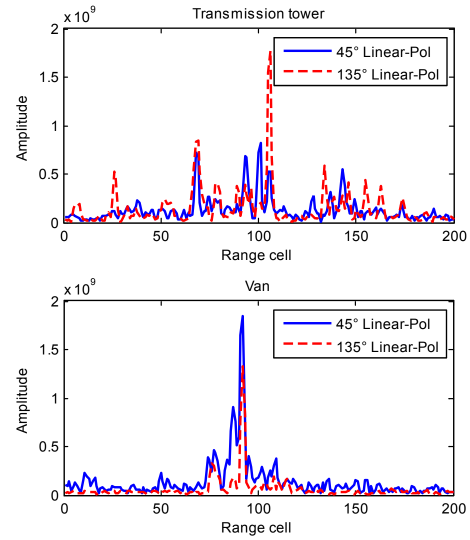

Fig. 6. Polarimetric HRRPs of the transmission tower and the van.

TABLE II. Proportion of Different Scattering Mechanisms

Type of Scattering mechanisms	**Proportion**	
	Transmission Tower	***Van***
Dihedral	37.88%	4.17%
Bragg	31.31%	64.58%
The 7 others	30.81%	31.25%

References

[1] D. H. Dai, B. Liao, S. P. Xiao and X. S. Wang, "Advancements on radar polarization information acquisition and processing," Journal of Radars, vol. 5, no. 2, pp. 143–155, April, 2016.

[2] X. S. Wang, "Status and prospects of radar polarimetry techniques," Journal of Radars, vol. 5, no. 2, pp. 119–131, April, 2016.

[3] H. C. Mac Donald, "Geological evaluation of radar imagery from Darien Province Panama," Modern Geology, vol. 1, pp. 1-62, February, 1969.

[4] J. J. van Zyl, H. A. Zebker and C. Elachi, "Imaging radar polarization signatures: Theory and observation," Radio Science, vol. 22, pp. 529–543, July, 1987.

[5] J. C. Souyris, P. Imbo, R. Fjortoft, Sandra Mingot and Jong-Sen Lee, "Compact polarimetry based on symmetry properties of geophysical media: the π/4 mode," IEEE Transactions on Geoscience and Remote Sensing, vol. 43, no. 3, pp. 634-646, March 2005.

[6] S. R. Cloude and E. Pottier, "A review of target decomposition theorems in radar polarimetry," IEEE Transactions on Geoscience and Remote Sensing, vol. 34, no. 2, pp. 498-518, March 1996.

[7] S. R. Cloude and E. Pottier, "An entropy based classification scheme for land applications of polarimetric SAR," IEEE Transactions on Geoscience and Remote Sensing, vol. 35, no. 1, pp. 68-78, January 1997.